Mechanisms of acclimation to hypersalinity in two European sea bass lineages: a focus on the kidney function

Quanquan Cao, Ivone Giffard-Mena, Eva Blondeau-Bidet, Sophie Hermet, Yau-Chung Hu, Tsung-Han Lee, Catherine Lorin-Nebel

Mechanisms of acclimation to hypersalinity in two European sea bass lineages: a focus on the kidney function

Quanquan CAO[1], Ivone GIFFARD-MENA[2], Eva BLONDEAU-BIDET[1], Sophie HERMET[1], Yau-Chung HU[3], Tsung-Han LEE[3], Catherine LORIN-NEBEL[1*]

[1]Univ Montpellier, MARBEC (CNRS, IFREMER, IRD, UM), 34095 Montpellier, France

[2]Universidad Autónoma de Baja California-Facultad de Ciencias Marinas, 22860 Ensenada, Baja California, Mexico

[3]Department of Life Sciences, National Chung Hsing University, Taichung, 402, Taiwan

***Corresponding author:**

Catherine LORIN-NEBEL

Univ Montpellier, MARBEC (CNRS, IFREMER, IRD, UM)

Place E. Bataillon,

34095 Montpellier cedex 05, France

Tel: +33 4 67 14 93 91

catherine.lorin@umontpellier.fr

Abstract

European sea bass (*Dicentrarchus labrax*), a major aquaculture species, is distributed along the coasts of the North-Eastern Atlantic Ocean, Mediterranean and Black Sea. *D. labrax* enter lagoons and estuaries where salinity fluctuates and sometimes reaches levels over 60 ‰, notably in Mediterranean lagoons. Keeping in mind that European sea bass are genetically subdivided in an Atlantic and a Mediterranean lineage, we compared fish from Atlantic (A) and West Mediterranean (M) populations regarding their capacity to tolerate hypersalinity with a focus on the kidney, a key organ involved in water reabsorption at high salinity. Fish were analyzed following a two-week transfer from seawater (SW, 36 ‰) to either seawater (SW, 36 ‰) or hypersaline water (HW, 55 ‰). Plasma osmolality was significantly increased in the MHW group compared to the other groups. Plasma sodium levels were significantly increased in hypersaline water compared to seawater in both lineages whereas plasma chloride levels showed an opposite trend. In order to estimate water filtration at the kidney level, the size of renal glomeruli was investigated and showed a decreased glomerulus perimeter and area in hypersaline water compared to seawater. NKA was highly expressed in all kidney tubules notably collecting tubules and ducts. There was an effect of salinity on renal *nka α1a* mRNA expression with slightly lower transcript levels at 55 ‰ compared to 36 ‰. Relative protein amounts and activity of NKA however were significantly higher in fish exposed to hypersalinity regardless of their origin. AQP1a immunolabeling differed between proximal tubules subtypes and only faint AQP1a was detected in subapical parts of cells lining collecting ducts. The transcript levels of renal *aqp 1a* were lower in the HW group than the SW group whereas the expression of other *aqp* paralogs (*aqp 1b*, *aqp 8b*) did not change according to the analyzed conditions. This study showed an efficient acclimation of sea bass to high salinity by increasing active ion transport at the kidney and by decreasing the size of filtering glomeruli to minimize water loss through urine. Despite Mediterranean *D. labrax* are supposed to more often encounter high salinities in their habitat, their high blood osmolality in hypersaline water indicates that their overall response to hypersalinity seems not improved compared to the Atlantic lineage. However, at the kidney level, the

traits analyzed differ slightly between genetic lineages, potentially as a response to high blood osmolalities in MHW.

Key words

Hypersalinity; Kidney; *Dicentrarchus labrax*; Intraspecific comparison; Osmoregulation

1. Introduction

European sea bass (*Dicentrarchus labrax*) are among the most important species for aquaculture production in Europe (Vandeputte et al. 2019). They mainly distribute along the coasts of the North-Eastern Atlantic Ocean and in Mediterranean and Black Sea. Throughout their distribution range, *D. labrax* adults and juveniles are found in a large variety of habitats such as the open sea, rocky shores, coastal lagoons, estuaries and rivers. Spawning occurs offshore whereas the transitory habitats are used for growth and as nurseries (Potts 1995). Two *D. labrax* lineages, Atlantic and Mediterranean, the latter subdivided into populations (Mediterranean East and West) have been characterized through genetic studies for around 25 years (Allegrucci et al. 1997, Caccone et al. 1997, Naciri et al. 1999, Duranton et al. 2018), but have received only few attention regarding physiological traits. Genetic variation between Atlantic and Mediterranean populations has shown impacts on responses triggered by abiotic factors or viral threats (Ayala et al. 2001, Person-Le Ruyet et al. 2004, Doan et al. 2017). Intraspecific variation in response to salinity change has been reported in different species regarding different phenotypic traits, i.e. ionoregulatory physiology in killifish (*Fundulus heteroclitus)* (Scott et al. 2004), swimming speed and metabolic rate in European perch (*Perca fluviatilis*) (Christensen et al. 2019), gene expression patterns of Na^+/K^+-ATPase and heat shock protein 70 in brown trout (*Salmo trutta*) (Larsen et al. 2008), salinity tolerance in the pike (*Esox lucius*) (Sunde et al. 2018) and freshwater tolerance in European sea bass (Nebel et al. 2005, L'Honoré et al. 2019, L'Honore et al. 2020). Mediterranean and Atlantic *D. labrax* live in close, slightly different salinities, at around 38 ‰ in the Mediterranean Sea (Yilmaz et al. 2020) and

36 ‰ in the Atlantic Ocean (Qu et al. 2013). In some Mediterranean lagoons, where *D. labrax* are found from spring to autumn, salinities are fluctuating and can reach values up to 60 ‰ in the summer (Dufour et al. 2009). In some coastal lagoons and saltpans of the Atlantic ocean, the salinity can also reach levels higher than 36 ‰ (Newton and Mudge 2003). To our knowledge, however, much less hypersaline areas are encountered by Atlantic *D. labrax*. The Mediterranean Sea is becoming more and more salty due to climate change (increased temperatures and evaporation) which points to the appearance of more hypersaline lagoons in the future (Borghini et al. 2014). The study of the fish's strategies to cope with high salinities is therefore of particular interest, notably in species entering coastal lagoons with increased salinities (Pérez-Ruzafa et al. 2005).

In high salinity environments, osmotic water loss in fish needs to be limited and/or compensated by water ingestion through an increased drinking rate (Aoki et al. 2003, Varsamos et al. 2004). Water reabsorption occurs mainly at the gastrointestinal tract and kidney. The kidney plays an essential role in divalent ion secretion (Donaldson et al. 1969). Proximal kidney tubules are responsible for $MgSO_4$ and water secretion whereas collecting and distal tubules are responsible for NaCl reabsorption followed by water in saltwater-acclimated fish (Cliff and Beyenbach 1992). To avoid dehydration in high salinities, the kidney produces thus less urine which is achieved by a decrease in glomerular filtration rate (Schmidt-Nielsen and Renfro 1975) and/or an increase in the permeability of renal tubules to reabsorb water together with ions from the urine to the blood. The salt gain needs then to be actively excreted from the body, mainly through the gills. The mesonephric kidney of most teleosts including *D. labrax* is not able to concentrate urine above plasma levels (Donaldson et al. 1969, Beyenbach 2004, Nebel et al. 2005). These ionic and osmoregulatory challenges escalate dramatically as environmental salinity increases beyond seawater to hypersaline levels (Gonzalez 2012).

Na^+/K^+-ATPase (NKA) is an ubiquitous membrane-bound ion-transporting enzyme that is fundamental to osmoregulation (Tomy et al. 2009). NKA actively pumps K^+ into and Na^+ out of a cell across the basolateral membrane through the hydrolysis of one molecule of ATP (Post and Jolly 1957). This enzyme creates an electrochemical gradient providing the driving force for sustaining internal

93 homeostasis associated with osmoregulatory function (Hwang and Lee 2007, McCormick et al. 2009). In
94 euryhaline teleosts, modulation of the activity or kinetics of NKA is essential notably in changing
95 environments (Gonzalez 2012). In our previous investigations on West Mediterranean *D. labrax*, we
96 measured a high *nka α1a* expression in the main osmoregulatory tissues (posterior kidney, gills and
97 intestine) compared to the much less expressed *nka α1b* (Blondeau-Bidet et al. 2016). Moreover, *nka α1a*
98 expression was significantly modulated according to salinity and seems thus to be a key player in
99 osmoregulatory processes. Transcript levels of *nka α1a* were higher in the kidney than posterior intestine
100 and gill after long-term (2.5 years) salinity acclimation in fresh water (FW) and seawater (SW). In the
101 kidney, short-term FW acclimation seemed to rapidly (within 1h) induce *nka α1a* and *nka α1b* transcript
102 levels followed by a decrease at 7 days and 24h, respectively, to pre-transfer levels (Blondeau-Bidet et al.
103 2016). Few data are available on the effect of hypersalinity on renal NKA expression in fish as most
104 studies focus on the response at gills and intestine levels (Gonzalez 2012, Li et al. 2014).
105 Numerous aquaporins have been characterized in fish, with up to twenty paralogous sequences in the
106 zebrafish *Danio rerio* (Finn et al. 2014). Aquaporins (AQPs) are transmembrane water channels with an
107 important function in whole-body and cellular water homeostasis (Martos-Sitcha et al. 2015). Aquaporin
108 1 has two paralogs (*aqp 1a* and *aqp 1b*) (Finn et al. 2014). Several studies refer to their expression in sea
109 water and/or freshwater media but only few of them address their expression in hypersaline media. In
110 zebrafish, *aqp 1a* is expressed in the kidney whereas *aqp 1b* seems not expressed in any osmoregulatory
111 organ (Tingaud-Sequeira et al. 2010). The transcript abundance of renal *aqp 1a* was found to be
112 unchanged among the different salinity groups (0, 6, 12, 33, 50 and 70 ‰) in silver sea bream (*Sparus*
113 *sarba*) for chronic salinity acclimation (1 month) (Deane et al. 2011). An et al. (2008) showed increased
114 levels of *aqp 1a* in the kidney of black porgy when transferred from FW to 10 ‰, whereas transfer to full
115 strength SW decreased the transcript level. In yellow European eels (*Anguilla anguilla)*, freshwater to
116 seawater acclimation reduced the transcript levels of the two *aqp 1* paralogs in the kidney (Martinez et al.
117 2005). In Atlantic salmon (*Salmo salar*), higher renal *aqp 1a* and lower *aqp 1b* levels were measured in
118 SW compared to FW (Tipsmark et al. 2010b). In a previous study conducted on West Mediterannean *D.*

119 *labrax*, renal and intestinal *aqp 1a* were highly expressed in seawater compared to fresh water (Giffard-
120 Mena et al. 2008) suggesting that AQP1a plays an important role in renal response to high-salinity media
121 in this species but it's subcellular localization has not been investigated.

122 Few data are available on aquaporin 8 in fish kidneys. Among the three *aqp 8* paralogs in zebrafish,
123 two were expressed at the kidney level: *aqp 8aa* and *aqp 8ab* (Tingaud-Sequeira et al. 2010). In marine
124 medaka (*Oryzias dancena*), *aqp 8* is higher expressed in FW than in SW (Kim et al. 2014) whereas no
125 change in expression was observed in Japanese medaka (*Oryzias latipes*) (Madsen et al. 2014). In Atlantic
126 salmon, *aqp 8b* mRNA levels increases at the parr-smolt transition in FW, but not protein levels
127 (Engelund and Madsen 2015). AQP8b is located in basolateral membranes of proximal tubules in this
128 species (Engelund and Madsen 2015). AQP8b, AQP1aa and AQP1ab are also expressed in membranes of
129 some proximal tubules in rainbow trout (*Oncorhynchus mykiss*) and not in distal tubules (Engelund and
130 Madsen 2011) and are potentially involved in fluid secretion as suggested for proximal tubules in several
131 species (Cliff and Beyenbach 1992, Beyenbach 2004, Martinez et al. 2005). These data clearly show
132 functional differences among aquaporin paralogs and species and a lack of data regarding the role of AQP
133 in salinities higher than seawater. It is crucial to better understand cellular and molecular mechanisms of
134 high salinity tolerance in order to evaluate how environmental change influences fish performance and
135 individual fitness.

136 The European sea bass provides an interesting model to study salinity tolerance and to compare
137 intraspecific differences in physiological capacities, as this species is an important aquaculture species
138 and wild populations are subdivided into two different genetic lineages that have evolved in habitats with
139 different salinity and temperature regimes which could lead to differential acclimation mechanisms
140 (Lemaire et al. 2005). Fish from Atlantic and West Mediterranean populations have been maintained in
141 aquaculture facilities. We address the question of how *D. labrax* respond to hypersalinity and whether
142 different lineages respond in the same way or not. Thus, the objectives of this study are i) to explore
143 hydromineral balance in *D. labrax* from two different lineages by analyzing plasma osmolality, Na^+ and

144 Cl^- as well as muscle water content in SW and hypersaline water, ii) to analyze glomerular size in *D.*
145 *labrax* kidney as a proxy for glomerular filtration, iii) to quantify expression of *nka α1*, *aqp 1* and *aqp 8*
146 paralogs; iv) to quantify specific activity of renal NKA, and v) to localize NKA and AQP1a in *D. labrax*
147 kidney. These analyses will be performed on European sea bass from West Mediterranean (M) and
148 Atlantic (A) origin acclimated to seawater (MSW, ASW, 36 ‰), or hypersaline water (MHW, AHW,
149 55 ‰) for two weeks. This study aims to a better understanding of the osmoregulatory strategies of
150 different *D. labrax* populations exposed to high salinities with a focus on the kidney.

151

152 **2. Materials and methods**

153 2.1 Experimental conditions and sampling

154 European sea bass *Dicentrarchus labrax* from West Mediterranean and Atlantic lineages (Vandeputte
155 et al. 2019) were obtained from the Ifremer Station at Palavas-les-Flots (Hérault, France).

156 Fish from both populations were brought to the Montpellier University and maintained for one week
157 in 3500 L tanks containing natural seawater from the Mediterranean Sea at 36 ‰, 20 °C and a constant
158 photoperiod 12hL/12hD. Fish were then transferred to smaller 200 L tanks containing either hypersaline
159 water (HW: 55 ‰) or seawater (SW: 36 ‰) and were maintained at this salinity for two weeks until
160 sampling. Four conditions were compared in this study: West Mediterranean *D. labrax* maintained at
161 36 ‰ (MSW) and 55 ‰ (MHW) and North Atlantic *D. labrax* maintained at 36 ‰ (ASW) and 55 ‰
162 (AHW). Water was aerated and mechanically/biologically filtered (Eheim System, Lens, Pas-de-Calais,
163 France). Hypersaline water was made by adding sea salt (Instant Ocean, Blacksburg, USA) to seawater.
164 Temperature, salinity, oxygen and nitrogen levels were regularly checked. 10% of the water was changed
165 regularly using a siphon tube. The tanks were then immediately refilled with water at the same salinity
166 and temperature (either SW or HW). Fish were fed with fish granules (Aphymar, Mèze, Hérault, France)
167 until 2 days before sampling. At the end of the experiment, fish were anesthetized in a solution of
168 benzocaine (50 ppm) prior to any manipulation. Fish mean fork length (FL) and body weight (W) have

been determined before sampling. A condition factor (CF) based on the fish fork length (FL) and the body wet weight (W) was calculated for fish of similar sizes as follow: $CF = 10^5 \, W \, FL^{-3}$. This index served to evaluate the length-weight relationship between fish (Le Cren, 1951). Blood was sampled from the caudal vessels using a 1-mL syringe coated with heparin (Li-heparin, Sigma-Aldrich, France) and fish were then killed by decapitation. For gene expression analysis and protein extraction, we collected the posterior kidney corresponding to one-third of the kidney length, sampled in the most posterior part of the kidney.

For mRNA analysis, tissues were collected in DNase- and RNase-free tubes and flash frozen using liquid nitrogen to be stored at −80 °C. For protein extraction, tissues were transferred into SEI buffer (300 mM sucrose, 20 mM Na_2EDTA, 100 mM imidazole, pH 7.4) containing compete EDTA-free proteinase inhibitors (Roche, Mannheim, Germany) and then frozen using liquid nitrogen to be stored at −80 °C. Posterior kidneys were collected at room temperature and transferred into Bouin's liquid for 48h for histology, then rinsed for several weeks in EtOH at 70%. The experiments were conducted according to the guidelines of the European Union (directive 86/609) and of the French law (decree 87/848) regulating animal experimentation.

2.2 Blood osmolality, plasma ion levels and muscle water content

Blood osmolality and plasma ions (Na^+ and Cl^-) were measured in 10-12 fish per condition. The osmolality of 20 µL of blood was measured on an Advanced 3300 micro-osmometer using an internal standard of 300 $mOsm \cdot kg^{-1}$. Plasma was obtained following centrifugation for 8 min at 10000g at 4 °C. 10 µL of plasma was used to determine chloride concentration using a chloride titrator (AMINCO, Maryland, USA) where a blank (0 $mEq \cdot L^{-1}$) and a standard solution (300 $mEq \cdot L^{-1}$) were used for calibration. Plasma sodium levels were determined by flame photometry (Sherwood, Cambridge, UK) using a standard curve of Na^+ from 0 to 400 $mEq \cdot L^{-1}$ and plasma at a 1/1000 dilution in MilliQ water. Na^+ and Cl^- levels were measured in duplicates. Muscle water content was determined as weight loss after drying a piece of muscle (ranging from 0.35 to 0.51g) cut near the fish tail in an oven at 105 °C for 72h. Values were expressed as percent wet weight.

195

196 2.3 mRNA extraction and complementary DNA (cDNA) synthesis

197 Total RNA was extracted from posterior kidneys using Nucleospin® RNA protocol (MACHEREY
198 NAGEL GMbH Co.KG, Germany) and processed according to the manufacturer's instructions. Following
199 DNAse treatment, RNA quantity was assessed by measuring the A260/A280 ratio using the NanoDrop®
200 One Spectrophotometer (ThermoFisher, USA). RNA was only used when the A260/A280 nm ratio was
201 above 1.9 and A260/A230 nm ratio was above 2.0. One microgram of isolated RNA was used to
202 synthesize first-strand cDNA using qScript™ cDNA SuperMix (Quanta Biosciences™) providing all
203 necessary components for first-strand synthesis, including oligo (dT) primers, random primers and
204 qScript reverse transcriptase. cDNA samples were stored at −20 °C.

205

206 2.4 Quantitative real-time RT-PCR (qRT-PCR)

207 The primers used in this study are indicated in Table 2. Ten to twelve fish per condition were analyzed
208 for gene expression studies. An Echo®525 liquid handling system (Labcyte Inc., San Jose, CA, USA)
209 was used to dispense 0.75 µL of SensiFAST™ SYBR® No-ROX Kit (Bioline, UK), 0.037 µL of each
210 primer (at 0.4 µM), 0.21 µL of ultra-pure water and 0.5 µL of diluted cDNA (diluted at 1/16) into a 384-
211 well reaction plate. The dilution of cDNA has been previously determined according to the standard
212 curves generated for each primer pair. Each sample was run in duplicates. The qRT-PCR conditions were
213 as follows: initial denaturation at 95 °C for 2.5 min, followed by 45 cycles of denaturation (95 °C, 15 s),
214 hybridization (60 °C, 5 s) and elongation (72 °C, 10 s), and a final step at 40 °C for 30 s. A melting curve
215 program was performed to control the amplification specificity. Ultra-pure water was used as a no-
216 template control in the qRT-PCR. Efficiencies were between 1.9 and 2.2 according to the considered
217 primer pair (Table 2). Expression levels were normalized to the geometric mean of three reference genes,
218 elongation factor (*ef1α*), ribosomal protein L13 (*l13*) and ribosomal protein S30 fusion gene (*fau*) with the
219 MSW condition as a control condition for the ΔΔCt calculation. Relative quantifications were performed

220 using the method of Vandesompele et al. (2002). Threshold cycle (Ct) of each of the three reference genes
221 did not vary according to the tested conditions (P<0.05).

222

223 2.5 Kidney histology, morphometric analyses and immunofluorescence

224 After extensive rinsing of posterior kidney tissues in 70% ethanol, samples were dehydrated in a
225 graded ethanol series to be embedded in Paraplast (Leica). Transverse sections (5 µm) were cut on a Leitz
226 Wetzlar microtome, collected on poly-L-lysine-coated glass slides and were stained using the Masson's
227 Trichrome staining protocol (Buzete Gardinal et al. 2019). Slides were observed under a Leica Diaplan
228 microscope and kidneys sections were photographed. For morphometric analyses, glomeruli area and
229 perimeter were measured using the Image J software (ImageJ ij152). In each condition, 3 animals have
230 been used and 11 measurements per animal have been done.

231 For immunolabeling of the Na^+/K^+-ATPase and AQP1a, sections were dewaxed (Histochoice),
232 hydrated through a descending series of ethanol baths (from 100% to 50%) and rinsed in phosphate-
233 buffered saline (PBS, pH 7.4, BioRad). Slides were then immersed for 10 min into 0.02% Tween 20, 150
234 mM NaCl in PBS, pH 7.3. After incubation in 5% bovine serum albumin (BSA) in PBS for 20 min, the
235 slides were rinsed three times with PBS. Primary labeling was performed for 2 h at room temperature in a
236 humidity chamber placed on a shaker with the following antibodies: mouse monoclonal antibody raised
237 against chicken Na^+/K^+-ATPase α5 (deposited to the Developmental Studies Hybridoma Bank by
238 Fambrough D.M. (DSHB Hybridoma Product α5), University of Iowa) and a polyclonal antibody
239 produced in rabbit raised against *D. labrax* AQP1a (Giffard-Mena et al. 2011) at 110 µg/ml in 0.5%
240 bovine serum albumin (BSA) in PBS. Negative control slides without the primary antibodies were also
241 prepared. After three washes in PBS to remove unbound antibody, the sections were incubated for 1 h
242 with a secondary antibody at 10 $\mu g \cdot mL^{-1}$ (goat anti-mouse Alexa Fluor 594, Invitrogen, Life
243 Technologies and Donkey anti-rabbit Alexa Fluor 488, Thermo Fisher Scientific). Following washes,
244 nuclei were counterstained with 4',6-diamidino-2-phenylindole (DAPI) during 2 min, and sections were

thoroughly washed in PBS and mounted in an anti-bleaching mounting medium (Immuno-histomount, Santa Cruz Biotechnology) to be observed with a Leica DM6B microscope equipped with a special filter set for fluorescence and coupled to a Leica DMC 2900 digital camera. Posterior kidney sections were photographed using objectives with a magnification of ×10, ×25 and ×40.

2.6 Protein extraction, NKA activity assay and immunoblotting

Posterior kidney tissues of fish stored at −80 °C in SEI buffer with proteinase inhibitors were thawed on ice for protein analysis. A Retsch Mixer mill MM400 (Haan, Germany) (frequency: 30 Hz, 1 min) was used for homogenization. After centrifugation at 1500 g (10 min at 4 °C), the supernatant containing the membranes was used for protein quantification (Bradford; Bio-Rad, France) and NKA activity measurements.

A colorimetric assay was used to measure the Na^+/K^+-ATPase activity based on the measurement of inorganic phosphate generated by the Na^+/K^+-ATPase with and without ouabain (Tang et al. 2010). 340 µL of reaction medium (final concentration: imidazole, 100 mM; NaCl, 125 mM; KCl, 75 mM; $MgCl_2$, 7.5 mM; pH 7.6) was mixed with 10 µL of protein sample (100 µg/µL), 2 mM Na_2ATP, and 0.5 mM ouabain (final concentrations) or deionized water. To test the potential of Na^+/K^+-ATPase activity, both groups were incubated in parallel at 37 °C for 20 min and the reaction was terminated in a freezer (-20 °C) for 10 min. The colorimetric reagent (final concentration: ammonium molybdate, 10 g/L; H_2SO_4, 0.9 M; Tween-20, 10 µL/mL) was mixed in equal volumes with the reaction samples, and inorganic phosphate was measured at 405 nm with a microplate reader (TECAN trading AG, Switzerland) to calculate Na^+/K^+-ATPase activity. The absorbance of each sample was determined in triplicate and a mean value was determined.

For immunoblotting, 5 µg of proteins were mixed with 0.4 µL β-mercaptoethanol and 3.6 µL loading buffer (Bio-Rad, Marnes la Coquette, Hauts-de-Seine, France). Then the proteins were separated by electrophoresis using sodium dodecyl sulfate-polyacrylamide gels (Bio-Rad, Marnes la Coquette, Hauts-de-Seine, France). Proteins were then transferred for 2·h on a PVDF membrane (WESTRAM Clear

Signal, Schleicher and Schuell, VWR, Val-de-Marne, France) using a wet transfer apparatus (Bio-Rad, Marnes la Coquette, Hauts-de-Seine, France). After transfer, the blots were incubated for 1 h in a commercial blocking buffer (LI-COR Biosciences, Lincoln, NE, USA). After rinsing with PBS, the blots were incubated at 4 °C overnight with the mouse monoclonal antibody Na^+/K^+-ATPase (α5) at 0.5 µg/mL, (Hybridoma Bank, University of Iowa) diluted in blocking buffer with Tween 20 (2 µL/mL), followed by rinsing and incubation with a secondary antibody, donkey anti-mouse Alexa Fluor® 800 (0.05 µL/mL, Invitrogen, Life Technologies) diluted in blocking buffer with Tween 20 (2 µL/mL) and 10% SDS. Following washes, immunoreactive bands were visualized and photographed using the Odyssey® Fc Imaging System (LI-COR Biosciences, Lincoln, NE, USA). The results were converted to numerical values to compare protein abundances of the immunoreactive bands (relative to one sample as a reference) using the software Image J (ImageJ ij152).

2.7 Statistical analyses

Statistical analyses were performed using GraphPad Prism (version 8, GraphPad Software Incorporated, La Jolla, CA 268, USA). Normality and homogeneity tests were verified using the D'Agostino-Pearson and Bartlett tests. If the data fit with these conditions, a two-way ANOVA analysis of variance with salinity and the lineages as main factors was performed followed by a Tukey's multiple comparisons test (Table 3). Conversely, if the normality and homogeneity of variances were not verified, Kruskal-Wallis test was performed followed by a Dunn's multiple comparisons test. Data are represented as box and whisker plots (from the first quartile to the third quartile) showing median, minimum and maximum values. Morphometrical data are represented using the mean +/- SD. Statistical differences were accepted at $P < 0.05$.

3. Results

295 *D. labrax* analyzed in this study were all characterized by a similar length and slight differences in
296 weight. Atlantic *D. labrax* were significantly heavier in hypersaline water than Mediterranean *D. labrax*
297 in seawater (Table 1). The mean condition factor (CF) however did not change significantly between
298 different conditions and was close to 1 (Table 1). Mortality was low with one death observed both in the
299 MSW and MHW group after 1 and 4 days of transfer.
300
301 3.1 Blood osmolality, muscle water content and plasma ion levels
302 In *D. labrax* maintained in SW (MSW and ASW), plasma osmolality was similar in all fish. After
303 transfer to hypersaline water, plasma osmolality was significantly increased in the MHW group but did
304 not change in the AHW group (Fig. 1A). Overall a significant salinity ($P<0.0001$), lineage ($P<0.001$) as
305 well as an interaction between those factors ($P<0.01$) was observed for osmolality. Plasma sodium levels
306 were significantly increased in hypersaline compared to seawater conditions for both Mediterranean and
307 Atlantic *D. labrax* lineages with a significant salinity effect ($P<0.0001$). Overall, plasma sodium levels
308 in Mediterranean *D. labrax* were higher than in Atlantic *D. labrax* notably at high salinity ($P<0.0001$)
309 (Fig. 1B). Plasma chloride levels were higher in seawater than in hypersaline water ($P<0.0001$) in
310 Atlantic *D. labrax* and to a lesser extent in Mediterranean *D. labrax* (Fig. 1C). Muscle water content was
311 slightly but not significantly higher in the MSW group compared to the other groups (Table 1).
312
313 3.2 Morphometric analysis and Na^+/K^+-ATPase α and Aquaporin 1a immunofluorescence in the kidney
314 Under light microscopy, distinct segments could be observed in the *D. labrax* kidney including
315 proximal tubules that are recognized by a narrow lumen and an apical brush border, collecting tubules,
316 large collecting ducts and glomeruli (Fig. 2 A-D). The size of kidney glomeruli has been estimated in
317 each condition by measuring the kidney glomerulus area (GA) and glomerulus perimeter (GP) (Fig. 2E,
318 F). The resulting data showed significantly higher values for GA (115-147% higher) and GP (139-230%
319 higher) in the MSW and ASW groups compared to the MHW and AHW groups (Fig. 2E, F) ($P<0.0001$).

No difference in GA and GP were detected between the three animals of the same condition (not shown), except for AHW were one animal (indicated by the blue dots) had a slightly higher GA than the animal indicated by green dots (Fig. 2E).

NKAα and AQP1a were labeled through immunofluorescence using kidney sections from at least 3 animals per condition. Control sections without primary antibody showed no immunolabeling (results not shown). No apparent difference was observed in NKAα and AQP1a immunolabeling between the four conditions (not shown). Glomeruli were not immunostained whatever the protein tested (Fig. 5). NKAα was detected through immunofluorescence in all urinary tubules and ducts of the different salinity groups of both lineages of European sea bass (Figs 5B, D, 6C, D). NKAα immunostaining was detected in the basolateral membrane of epithelial cells of all observed renal tubules with some differences. Collecting tubules and ducts showed a much stronger NKAα immunostaining and the immunolabeled area seemed to be more thoroughly distributed in the whole cell (Figs 5B, D, 6C, D).

AQP1a immunostaining clearly differs among renal tubule types in all fish analyzed (for MSW, see Fig. 5A). Two types of proximal tubules could be distinguished through their differential immunostaining (Fig. 5E), generally referred to as proximal tubule I and II. The proximal tubule type that we call proximal tubule II (according to Islam et al., 2013), with a strong basolateral NKAα staining and a very faint AQP1a staining, is less abundant (Fig. 5D, E, labeled '*'). The other proximal tubule type that we call proximal tubule I, is more abundant and shows a strong basolateral AQP1a staining and a weak basolateral NKAα staining. It is labeled as '+' in Fig. 5. Distal tubules are recognized by an epithelium without apical brush border and are strongly stained in the whole cells for NKAα whereas AQP1a is nearly not detectable (Fig. 5A, D, E arrows). Collecting ducts comprise huge cells (around 20µm long) with a strong NKAα staining throughout the cell (Fig. 6C, D) and a faint subapical AQP1a staining, probably present in subapical vesicles (Fig. 6B).

3.3 Na^+/K^+-ATPase and aquaporin 1 and 8 mRNA expression in the posterior kidney

345 In the posterior kidney, *nka α1a* mRNA levels were slightly higher in SW compared to HW in both
346 lineages (Salinity effect: $P<0.01$) (Fig. 3A). There was also an effect of the lineage with higher values in
347 Mediterranean vs Atlantic *D. labrax* ($P<0.01$). Regarding *nka α1b*, a significant higher expression was
348 observed in MHW compared to MSW and an overall salinity effect ($P<0.05$). No obvious difference was
349 observed between salinities in the Atlantic lineage (Fig. 3B). The mRNA levels of *aqp 1a* were
350 significantly higher in seawater- compared to hypersaline-acclimated individuals of both lineages (Fig.
351 3C) (Salinity effect: $P<0.001$) and an overall higher level of *aqp 1a* was observed in Mediterranean fish
352 (Lineage effect: $P<0.01$). Regarding *aqp 1b*, no differences were observed among all groups (Fig. 3D).
353 The three paralogs, *aqp 8a*, *aqp 8ab* and *aqp 8b* were measured in the kidney but *aqp 8aa* and *aqp 8ab*
354 expression was not detectable. No difference among groups has been measured in *aqp 8b* mRNA
355 expression (Fig. 3E) with however a slight lineage effect ($P<0.05$).
356
357 3.4 Na^+/K^+-ATPase protein level and activity
358 Immunoblots showed one single band for NKA at about 105 kDa in each condition (Fig. 4A). Relative
359 Na^+/K^+-ATPase protein levels were quantified, and the hypersaline-acclimated individuals showed
360 significantly higher NKA protein levels than the SW-acclimated individuals of both lineages (Fig. 4B)
361 (Salinity effect: $P<0.0001$). Comparisons between *D. labrax* lineages showed lower and less variable
362 NKA protein levels in the AHW group compared to the MHW group (Lineage effect: $P<0.0001$). The
363 pattern of renal NKA specific activity was similar to that of protein abundance with higher NKA activity
364 in hypersaline conditions compared to SW (Fig. 4C) (Salinity effect: $P<0.0001$). In addition, lower NKA
365 activity was measured in ASW group compared to MSW group (Lineage effect: $P<0.01$).
366
367 ## 4. Discussion
368 The subdivision of the European sea bass into two genetic lineages, an Atlantic and a Mediterranean
369 lineage, structured into populations within the Mediterranean Sea (Naciri et al. 1999, Bahri-Sfar et al.

2000, Quéré et al. 2012) raises the question if fish differentially respond to environmental change. As a main aquaculture species and in the context of climate change, it is crucial to analyze in each lineage the physiological and molecular traits involved in the response to salinity changes, notably at high salinities.

Hydromineral balance is differently regulated between two lineages of European sea bass

Our results showed that hydromineral balance is differently regulated between both lineages when transferred directly to hypersalinity with the Atlantic lineage having a more pronounced decrease in plasma Cl^- levels than the Mediterranean lineage. The fact that Mediterranean *D. labrax* have significantly higher Na^+ levels in HW than the Atlantic lineage explain the maintenance of blood osmolality in Atlantic *D. labrax* whereas West Mediterranean *D. labrax* have a significantly higher blood osmolality at 55 ‰ compared to SW. In a previous study performed in European sea bass whose genetic lineage was not known, plasma osmolality and Na^+ have been shown to increase after a ten-day transfer from 15 ‰ to hypersaline water at 50 ‰ (Jensen et al. 1998). In the latter study, plasma Na^+ and Cl^- levels at 50 ‰ were at about 200 mmol/L and 160 mmol/L, respectively, which is close to our results in Mediterranean *D. labrax* at 55 ‰ (MHW). The fact to have performed a direct and not a gradual salinity transfer might be the reason of increased blood osmolality in MHW. If this is the case, Mediterranean *D. labrax* would respond less efficiently to direct changes in salinity than Atlantic *D. labrax* which was not expected. Acclimation capacity to high salinity can be enhanced following gradual transfer as shown in 'California' tilapia hybrids (Sardella et al. 2004) and should be tested in both *D. labrax* lineages. According to Gonzalez (2012), a transfer to hypersalinity below 70 ‰ does not affect blood osmolality in several euryhaline marine species as shown in the Atlantic *D. labrax*, gulf toadfish (*Opsanus beta*) (McDonald and Grosell 2006) and the gilthead sea bream (*Sparus auratus*) (Sangiao-Alvarellos et al. 2005). An increase in plasma Na^+ content following transfer from SW to hypersaline water has been shown in various teleostean species (Sardella et al. 2004, Gonzalez et al. 2005, McDonald and Grosell 2006, Genz et al. 2011, Malakpour et al. 2018). In 'California' tilapia hybrids, a time-course analysis showed increased Cl^- levels at 65 ‰ at 24h post-transfer followed by a progressive decrease to pre-

transfer levels at 5 days (Sardella et al. 2004). The slightly decreased plasma Cl^- levels in our study is rather surprising and unique, suggesting efficient Cl^- secretion mechanisms in European sea bass of both genetic lineages. Cl^- transport is known to be coupled to HCO_3^- transport mechanisms through either anion exchanger 1 or solute carrier family 26 exchangers *slc26a6* exchangers and therefore also depends on acid-base regulatory mechanisms (Evans et al., 2005). Salinity changes can affect plasma pH levels in juvenile *D. labrax* as shown previously by Masroor et al. (2019) which could trigger the expression and activation of transporters involved in the regulation of acid-base balance. At least two *slc26a* paralogous genes are highly expressed in *D. labrax* gill and renal tissues at high salinity, *slc26a6c* and *slc26a6a* respectively (L'Honoré et al., 2019). The role and involvement of these proteins in chloride homeostasis and pH regulation should be investigated in future studies upon hypersalinity acclimation.

Significant decreases in the muscle water content at higher salinity have been reported in many fish species (Jensen et al. 1998, McDonald and Grosell 2006, Malakpour et al. 2018). In our study, muscle water content was slightly lower in hypersaline water compared to seawater but with no significant differences among the four tested groups. This remarkable stability in muscle water content in hypersaline water suggests efficient cell volume regulatory mechanisms contributing to the strong euryhalinity of this species. .

Renal NKA expression upon high salinity transfer

In the previous reports in *D. labrax*, short-term FW acclimation seemed to rapidly increase *nka α1a* transcript levels in the kidney but no difference between SW and FW was observed after seven days (Blondeau-Bidet et al. 2016). In the present study, the salinity had an effect after long term hypersalinity transfer but when lineages where considered separately, this salinity effect was not significant neither for the Atlantic ($P<0.151$) nor the Mediterranean lineage ($P<0.056$). Previous investigations have shown that *nka α1b* is less expressed than *nka α1a* in all osmoregulatory tissues (Blondeau-Bidet et al. 2016) which is also the case in the present study (not shown). It is worth noting that there is a similar tendency

in *nka α1b* expression, NKA α-subunit content and specific enzyme activity. In Mediterranean *D. labrax* challenged to high salinities, these three traits show the highest levels compared to the other conditions. This might be part of the response to the high osmolality in these fish but further investigations are necessary to confirm this statement. Overall, NKA activity and relative protein amounts were higher in *D. labrax* exposed to hypersalinity of both considered populations. However, we were not able to determine through immunocytochemistry what tubule section expressed more NKA in HW compared to SW. However, the tubules that highly express NKA did not express AQP1a, as distal tubules and collecting ducts as well as proximal tubule II. To have a better insight of which tubule section express what gene, other methods should be used, for example laser capture micro-dissections as done recently in Atlantic salmon *S. salar* (Madsen et al., 2020). In a previous study, renal NKA activity and α-subunit abundance have been measured and were higher in the FW group compared to the SW group (Nebel et al. 2005) which suggests an 'U-shaped' salinity response of NKA protein levels and activity with high levels at extreme salinities (FW and HW) as previously shown at the gill level (Jensen et al. 1998). In the kidney of the striped eel catfish, NKA activity was significantly higher in HW (60 ‰) than in SW (34 ‰) following a 2 week challenge, but transcript levels did not change significantly (Malakpour et al. 2018), which is similar to our results. In black porgy *Acanthopagrus schlegeli*, however, no difference in renal NKA activity was shown at different salinities (0, 5, 15, 33, 45 ‰) (Tomy et al. 2009) as well as in the euryhaline milkfish *Chanos chanos* between SW and 60 ‰ (Tang et al., 2010). It is clear that NKA expression profiles following salinity challenge vary between teleost species and can even slightly change between populations as shown in this study. The inconsistency found between mRNA and protein levels may be due to posttranscriptional changes in protein expression (Tipsmark et al. 2010a, Yang et al. 2016). Moreover, a time-course analysis is necessary to fully understand *nka α1* expression patterns and relate them to protein levels at high salinities.

NKA was highly expressed in collecting tubules and ducts of both *D. labrax* lineages in SW and hypersaline water. Renal NKA was also distributed in proximal tubules but with slightly different intensities among tubule types, and not in the filtering glomeruli as previously shown in SW and FW

447 (Nebel et al. 2005). For marine fishes, the collecting and distal tubules appear to be the site of
448 reabsorption of monovalent ions and organic compounds (Madsen et al. 2015). Active ion reabsorption
449 enabled by NKA is often coupled to an osmotic water transport to the blood, depending on the water
450 permeability of the urinary epithelium (Hickman and Trump 1969).
451
452 **The importance of kidney in maintaining water balance upon high salinity transfer**
453 The kidney plays a critical role in maintaining water balance following salinity change notably
454 through the modification of key renal structures. At high environmental salinity, fish need to activate
455 tubular water reabsorption from the urine (McDonald 2007) and decrease their glomerular filtration rate
456 in order to avoid dehydration and to produce more concentrated urine than in fresh water (Nebel et al.
457 2005, Janech et al. 2006). Decreasing the number and size of filtering glomeruli appears thus to be an
458 indicator of decreased glomerular filtration (Hasan et al. 2017). Hypersalinity significantly affected the
459 size of renal glomeruli in *D. labrax* indicating a decreased glomerular filtration contributing to avoid
460 dehydration. As muscle water content is maintained constant between salinity conditions, *D. labrax* do
461 not seem to suffer dehydration. Even if the decrease in glomerular area and perimeter seem more
462 pronounced in the Mediterranean lineage, no clear population-related difference in the capacity of
463 remodeling glomerular diameter has been shown in European sea bass, contrary to previous studies
464 performed in two stickleback populations that have evolved in different salinity environments and where
465 high salinity differently affects the glomerulus diameter (Hasan et al. 2017). European sea bass from
466 Atlantic and Mediterranean lineages have evolved in only slightly different salinities, respectively 36 ‰
467 and 38 ‰ and high salinities (>50 ‰) were experienced only in some Mediterranean lagoons (Chervinski
468 1975, Pérez-Ruzafa et al. 2005, Borghini et al. 2014).
469 Water reabsorption by the kidney is facilitated by the presence of aquaporins embedded in the cell
470 membranes. In European sea bass, a clear decrease in *aqp 1a* levels was shown in hypersaline-acclimated
471 fish compared to SW while no difference was found for *aqp 1b*. The transcription of both *aqp1* paralogs
472 is thus differently triggered at high salinities. The fact that different *aqp 1* paralogs do not respond the

same way following salinity challenge has previously been shown in other species (Tipsmark et al. 2010b) and differences in *aqp 1* expression seems to be species specific (Deane et al. 2011). When European eels (*Auguilla anguilla)* were acclimated to SW, renal expression of *aqp 1b* decreased after 21 days SW exposure from FW (Cerdà and Finn 2010). On the contrary, renal *aqp 1b* transcript amounts of Atlantic salmon were found to be significantly lower in fresh water compared to seawater (Tipsmark et al. 2010b).

In the kidney of eels, AQP1 was localized in the apical brush border of proximal, rather than distal tubule cells, and accordingly the authors suggested that AQP1 is involved in fluid secretion in early sections of the tubule (Martinez et al. 2005). There is also evidence of AQP1 in the vascular endothelium of the kidney, suggesting a further role in fluid transport to the blood (Tipsmark et al. 2010b). In this study, two types of proximal tubules were identified with probably different functions. This is the first evidence in the kidney of European sea bass showing the presence of two types of proximal tubules. Proximal tubule II has a well-developed apical brush border and a strong immunostaining for NKA (Islam et al. 2013) seems not involved in transepithelial water transport using AQP1A due to its low immunostaining. Other aquaporins should be investigated in order to determine if transepithelial water transport occurs in these tubule sections. Proximal tubule I in contrast has a strong basolateral AQP1a staining, but low NKAα and seems to be involved in water transport between the blood and the cells, potentially to regulate cell volume or water balance. The low NKAα immunolabeling in those tubules indicates a less active ion transport than in proximal tubules II. Water transport in fact parallels ion transport (Cliff and Beyenbach 1992). As the main function of collecting tubules is ion reabsorption (notably NaCl), aquaporin expression in those tubules would enhance water absorption to the blood which could help to avoid dehydration at high salinity. In Atlantic salmon, *Salmo salar*, a high expression of *aqp1aa* and *aqp1ab* has been measured in distal versus proximal tubules (Madsen et al., 2020). This seems not the case in *D. labrax* AQP1a as its protein expression in collecting tubules and ducts is very low and it seems not to be localized in membranes. The precise role of AQP1a in proximal tubules I remains to be further analyzed. AQP8 might have a different role and localization, even though this protein has been detected in proximal tubules in other species. Among the three *aqp 8* paralogs, only *aqp*

8b could be detected, contrary to other species like zebrafish (Tingaud-Sequeira et al. 2010), Japanese medaka (Madsen et al. 2014), marine medaka (Kim et al. 2014) and Atlantic salmon (Madsen et al., 2020). In *D. labrax*, no difference in *aqp 8b* mRNA levels was observed among tested groups suggesting that either its renal expression is not regulated in response to salinity, as already stated by Madsen et al. (2015), or its expression is differently handled by different tubule sections (Madsen et al., 2020) which needs to be further explored.

Conclusion

This study is the first to demonstrate physiological and molecular responses to hypersalinity between European sea bass lineages. The Atlantic lineage maintains stable blood osmolalities at 55 ‰, which points to a more effective response towards excessive ion charges compared to the Mediterranean lineage. At the kidney level, the glomerular size was decreased at this high salinity in order to minimize water loss through urine. NKA was highly expressed in collecting ducts of all fish, but AQP1a does not contribute to water reabsorption at distal levels. NKA renal activity and relative protein amounts were higher in fish exposed to hypersalinity suggesting increased active ion transport, more pronounced in the Mediterranean lineage, probably linked to an increased need to excrete ions.

Acknowledgements

The authors would like to thank Dr. François Allal and the Ifremer team at Palavas-les-Flots for providing European sea bass lineages from Atlantic and West Mediterranean origin. The authors also thank the qPCR CeMEB (Centre Méditerranée en Environnement et Biodiversité) platform. This work has benefited from facilities funded by the 2015-2020 CPER CELIMER (French Ministry of Higher Education, Research and Innovation, Occitanie Region, Montpellier Mediterranée Metropolis, Sète Agglopole Méditerranée, Ifremer, IRD). This study was partially supported by the Taiwan-France

ORCHID (MOST-108-2911-I-005-507 and PHC ORCHID 2020-42971XC, BFT, MEAE, MESRI) grants to T.H.L. and C.L.N.

References

Allegrucci, G., Fortunato, C., Sbordoni, V., 1997. Genetic structure and allozyme variation of sea bass (*Dicentrarchus labrax* and *D. punctatus*) in the Mediterranean Sea. Mar. Biol. 128(2), 347-358.

An, K.W., Kim, N.N., Choi, C.Y., 2008. Cloning and expression of aquaporin 1 and arginine vasotocin receptor mRNA from the black porgy, *Acanthopagrus schlegeli*: effect of freshwater acclimation. Fish. Physiol. Biochem. 34(2), 185-194.

Aoki, M., Kaneko, T., Katoh, F., Hasegawa, S., Tsutsui, N., Aida, K., 2003. Intestinal water absorption through aquaporin 1 expressed in the apical membrane of mucosal epithelial cells in seawater-adapted Japanese eel. J. Exp. Biol. 206(19), 3495-3505.

Ayala, M.a.D., López-Albors, O., Gil, F., García-Alcázar, A., Abellán, E., Alarcón, J.A., Álvarez, M.a.C., Ramírez-Zarzosa, G., Moreno, F., 2001. Temperature effects on muscle growth in two populations (Atlantic and Mediterranean) of sea bass, *Dicentrarchus labrax*. Aquaculture 202(3), 359-370.

Bahri-Sfar, L., Lemaire, C., Hassine, O.K.B., Bonhomme, F., 2000. Fragmentation of sea bass populations in the western and eastern Mediterranean as revealed by microsatellite polymorphism. Proc. R. Soc. London, Ser. B 267(1446), 929-935.

Beyenbach, K.W., 2004. Kidneys sans glomeruli. Am. J. Physiol. Renal. Physiol. 286(5), F811-827.

Blondeau-Bidet, E., Bossus, M., Maugars, G., Farcy, E., Lignot, J.H., Lorin-Nebel, C., 2016. Molecular characterization and expression of Na^+/K^+-ATPase α1 isoforms in the European sea bass *Dicentrarchus labrax* osmoregulatory tissues following salinity transfer. Fish. Physiol. Biochem. 42(6), 1647-1664.

Borghini, M., Bryden, H., Schroeder, K., Sparnocchia, S., Vetrano, A., 2014. The Mediterranean is becoming saltier. Ocean Sci. 10(4), 693-700.

Buzete Gardinal, M.V., Rocha Ruiz, T.F., Estevan Moron, S., Oba Yoshioka, E.T., Uribe Goncalves, L., Franceschini Vicentini, I.B., Vicentini, C.A., 2019. Heart structure in the Amazonian teleost *Arapaima gigas* (Osteoglossiformes, Arapaimidae). J. Anat. 234(3), 327-337.

Caccone, A., Allegrucci, G., Fortunato, C., Sbordoni, V., 1997. Genetic differentiation within the European sea bass (*Dicentrarchus labrax*) as revealed by RAPD-PCR assays. J. Hered. 88(4), 316-324.

Cerdà, J., Finn, R.N., 2010. Piscine aquaporins: an overview of recent advances. J. Exp. Zool. A 313(10), 623-650.

Chervinski, J., 1975. Sea basses, *Dicentrarchus labrax* (Linné) and *D. punctatus* (Bloch) (Pisces, Serranidae), a control fish in fresh water. Aquaculture 6(3), 249-256.

Christensen, E.A.F., Stieglitz, J.D., Grosell, M., Steffensen, J.F., 2019. Intra-specific difference in the effect of salinity on physiological performance in european perch (*Perca fluviatilis*) and its ecological importance for fish in estuaries. Biology 8(4), 89.

Cliff, W.H., Beyenbach, K.W., 1992. Secretory renal proximal tubules in seawater- and freshwater-adapted killifish. Am. J. Physiol. 262(1), F108- F116.

Deane, E.E., Luk, J.C.Y., Woo, N.Y.S., 2011. Aquaporin 1a expression in gill, intestine, and kidney of the euryhaline silver sea bream. Front. Physiol. 2 (39).

Doan, K., Vandeputte, M., Chatain, B., Haffray, P., Vergnet, A., Breuil, G., Allal, F., 2017. Genetic variation of resistance to viral nervous necrosis and genetic correlations with production traits in wild populations of the European sea bass (*Dicentrarchus labrax*). Aquaculture 478, 1-8.

Donaldson, H.a., Holmes, W.W., Donaldson, E.M., 1969. Excretion, ionic regulation, and metabolism, in: Hoar, W.S., Randall D.J. (Eds.), Fish Physiology, vol. 1. Academic Press, New York, pp. 1-465.

Dufour, V., Cantou, M., Lecomte, F., 2009. Identification of sea bass (*Dicentrarchus labrax*) nursery areas in the north-western Mediterranean Sea. J. Mar. Biolog. 89(7), 1367-1374.
Duranton, M., Allal, F., Fraïsse, C., Bierne, N., Bonhomme, F., Gagnaire, P.-A., 2018. The origin and remolding of genomic islands of differentiation in the European sea bass. Nat. Commun. 9(1), 2518.
Engelund, M.B., Madsen, S.S., 2011. The role of aquaporins in the kidney of euryhaline teleosts. Front. Physiol. 2, 51.
Engelund, M.B., Madsen, S.S., 2015. Tubular localization and expressional dynamics of aquaporins in the kidney of seawater-challenged Atlantic salmon. J. Comp. Physiol. B 185(2), 207-223.
Evans, D. H., Piermarini, P. M., Choe, K. P., 2005. The multifunctional fish gill: dominant site of gas exchange, osmoregulation, acid-base regulation, and excretion of nitrogenous waste. Physiol. Rev. 85(1), 97-177.
Finn, R.N., Chauvigne, F., Hlidberg, J.B., Cutler, C.P., Cerda, J., 2014. The lineage-specific evolution of aquaporin gene clusters facilitated tetrapod terrestrial adaptation. PLoS One 9(11), e113686.
Genz, J., McDonald, M.D., Grosell, M., 2011. Concentration of $MgSO_4$ in the intestinal lumen of Opsanus beta limits osmoregulation in response to acute hypersalinity stress. Am. J. Physiol. 300(4), R895-909.
Giffard-Mena, I., Boulo, V., Abed, C., Cramb, G., Charmantier, G., 2011. Expression and localization of aquaporin 1a in the sea-bass (*Dicentrarchus labrax*) during ontogeny. Front. Physiol. 2, 34.
Giffard-Mena, I., Lorin-Nebel, C., Charmantier, G., Castille, R., Boulo, V., 2008. Adaptation of the sea-bass (*Dicentrarchus labrax*) to fresh water: role of aquaporins and Na^+/K^+-ATPases. Comp. Biochem. Physiol. A 150(3), 332-338.
Gonzalez, R.J., 2012. The physiology of hyper-salinity tolerance in teleost fish: a review. J. Comp. Physiol. B 182(3), 321-329.
Gonzalez, R.J., Cooper, J., Head, D., 2005. Physiological responses to hyper-saline waters in sailfin mollies (*Poecilia latipinna*). Comp. Biochem. Physiol. A 142(4), 397-403.
Hasan, M.M., DeFaveri, J., Kuure, S., Dash, S.N., Lehtonen, S., Merilä, J., McCairns, R.J.S., 2017. Sticklebacks adapted to divergent osmotic environments show differences in plasticity for kidney morphology and candidate gene expression. J. Exp. Biol. 220(12), 2175-2186.
Hickman, C.P., Trump, B.F., 1969. The kidney, in: Hoar, W.S., Randall, D.J (Eds.), Fish Physiology, vol I. Academic Press, New York, pp 91–239.
Hwang, P.P., Lee, T.-H., 2007. New insights into fish ion regulation and mitochondrion-rich cells. Comp. Biochem. Physiol. A 148(3), 479-497.
Islam, Z., Hayashi, N., Yamamoto, Y., Doi, H., Romero, M.F., Hirose, S., Kato, A., 2013. Identification and proximal tubular localization of the Mg^{2+} transporter, Slc41a1, in a seawater fish. Am. J. Physiol. 305(4), R385-R396.
Janech, M.G., Fitzgibbon, W.R., Ploth, D.W., Lacy, E.R., Miller, D.H., 2006. Effect of low environmental salinity on plasma composition and renal function of the Atlantic stingray, a euryhaline elasmobranch. Am. J. Physiol. 291(4), F770-F780.
Jensen, M.K., Madsen, S.S., Kristiansen, K., 1998. Osmoregulation and salinity effects on the expression and activity of Na^+,K^+-ATPase in the gills of European sea bass, *Dicentrarchus labrax*. J. Exp. Zool. 282(3), 290-300.
Kim, Y.K., Lee, S.Y., Kim, B.S., Kim, D.S., Nam, Y.K., 2014. Isolation and mRNA expression analysis of aquaporin isoforms in marine medaka *Oryzias dancena*, a euryhaline teleost. Comp. Biochem. Physiol. A 171, 1-8.
L'Honoré, T., Farcy, E., Blondeau-Bidet, E., Lorin-Nebel, C., 2020. Inter-individual variability in freshwater tolerance is related to transcript level differences in gill and posterior kidney of European sea bass. Gene 741, 144547.
L'Honoré, T., Farcy, E., Chatain, B., Gros, R., Ruelle, F., Hermet, S., Blondeau-Bidet, E., Naudet, J., Lorin-Nebel, C., 2019. Are European sea bass as euryhaline as expected? Intraspecific variation in freshwater tolerance. Mar. Biol. 166(8), 102. https://doi.org/10.1007/s00227-019-3551-z

Larsen, P.F., Nielsen, E.E., Koed, A., Thomsen, D.S., Olsvik, P.A., Loeschcke, V., 2008. Interpopulation differences in expression of candidate genes for salinity tolerance in winter migrating anadromous brown trout (*Salmo trutta L.*). BMC Genet. 9, 12.
Le Cren E. D., 1951. The length-weight relationship and seasonal cycle in gonad weight and condition in the perch (*Perca fluviatilis*). J. Anim. Ecol. 201-219.
Lemaire, C., Versini, J.J., Bonhomme, F., 2005. Maintenance of genetic differentiation across a transition zone in the sea: discordance between nuclear and cytoplasmic markers. J. Evol. Biol. 18(1), 70-80.
Li, Z., Lui, E.Y., Wilson, J.M., Ip, Y.K., Lin, Q., Lam, T.J., Lam, S.H., 2014. Expression of key ion transporters in the gill and esophageal-gastrointestinal tract of euryhaline Mozambique tilapia *Oreochromis mossambicus* acclimated to fresh water, seawater and hypersaline water. PLoS One 9(1), e87591.
Madsen, S.S., Bollinger, R.J., Brauckhoff, M., Engelund, M.B., 2020. Gene expression profiling of proximal and distal renal tubules in Atlantic salmon (*Salmo salar*) acclimated to fresh water and seawater. Am. J. Physiol. 319(3), F380-F393.
Madsen, S.S., Bujak, J., Tipsmark, C.K., 2014. Aquaporin expression in the Japanese medaka (*Oryzias latipes*) in freshwater and seawater: challenging the paradigm of intestinal water transport? J. Exp. Biol. 217(17), 3108-3121.
Madsen, S.S., Engelund, M.B., Cutler, C.P., 2015. Water transport and functional dynamics of aquaporins in osmoregulatory organs of fishes. Biol. Bull. 229(1), 70-92.
Malakpour, K.S., Coimbra, J., Wilson, J.M., 2018. Osmoregulation in the *Plotosidae Catfish*: role of the salt secreting dendritic organ. Front. Physiol. 9, 761.
Martinez, A.S., Cutler, C.P., Wilson, G.D., Phillips, C., Hazon, N., Cramb, G., 2005. Cloning and expression of three aquaporin homologues from the European eel (*Anguilla anguilla*): effects of seawater acclimation and cortisol treatment on renal expression. Biol. Cell 97(8), 615-627.
Martos-Sitcha, J.A., Campinho, M.A., Mancera, J.M., Martínez-Rodríguez, G., Fuentes, J., 2015. Vasotocin and isotocin regulate aquaporin 1 function in the sea bream. J. Exp. Biol. (5), 684-693.
Masroor, W., Farcy, E., Blondeau-Bidet, E., Venn, A., Tambutté, E., Lorin-Nebel, C., 2019. Effect of salinity and temperature on the expression of genes involved in branchial ion transport processes in European sea bass. J. Therm. Biol. 85, 102422.
McCormick, S.D., Regish, A.M., Christensen, A.K., 2009. Distinct freshwater and seawater isoforms of Na^+/K^+-ATPase in gill chloride cells of Atlantic salmon. J. Exp. Biol. 212(24), 3994-4001.
McDonald, M., 2007. The renal contribution to salt and water balance, in: Baldisserotto, J.M., Romero, B., Kapoor, G. (Eds.), Fish osmoregulation. Science Publishers., Enfield, pp. 322–345.
McDonald, M.D., Grosell, M., 2006. Maintaining osmotic balance with an aglomerular kidney. Comp. Biochem. Physiol. A 143(4), 447-458.
Naciri, M., Lemaire, C., Borsa, P., Bonhomme, F., 1999. Genetic study of the Atlantic/Mediterranean transition in sea bass (*Dicentrarchus labrax*). J. Hered. 90(6), 591-596.
Nebel, C., Romestand, B., Negre-Sadargues, G., Grousset, E., Aujoulat, F., Bacal, J., Bonhomme, F., Charmantier, G., 2005. Differential freshwater adaptation in juvenile sea-bass *Dicentrarchus labrax*: involvement of gills and urinary system. J. Exp. Biol. 208(20), 3859-3871.
Newton, A., Mudge, S.M., 2003. Temperature and salinity regimes in a shallow, mesotidal lagoon, the Ria Formosa, Portugal. Estuarine Coastal Shelf Sci. 57(1), 73-85.
Pérez-Ruzafa, A., Fernández, A.I., Marcos, C., Gilabert, J., Quispe, J.I., García-Charton, J.A., 2005. Spatial and temporal variations of hydrological conditions, nutrients and chlorophyll a in a Mediterranean coastal lagoon (Mar Menor, Spain). Hydrobiologia 550(1), 11-27.
Person-Le Ruyet, J., Mahé, K., Le Bayon, N., Le Delliou, H., 2004. Effects of temperature on growth and metabolism in a Mediterranean population of European sea bass, *Dicentrarchus labrax*. Aquaculture 237(1-4), 269-280.
Post, R.L., Jolly, P.C., 1957. The linkage of sodium, potassium, and ammonium active transport across the human erythrocyte membrane. Biochim. Biophys. Acta 25(1), 118-128.

668 Potts, G., 1995. Sea bass. Biology, exploitation and conservation, G. D. Pickett and M. G. Pawson,
669 Chapman & Hall. Aquat. Conserv.: Mar. Freshw. Ecosyst. 5(2), 167-168.
670 Qu, T., Gao, S., Fukumori, I., 2013. Formation of salinity maximum water and its contribution to the
671 overturning circulation in the North Atlantic as revealed by a global general circulation model. J.
672 Geophys. Res. Oceans 118(4), 1982-1994.
673 Quéré, N., Desmarais, E., Tsigenopoulos, C.S., Belkhir, K., Bonhomme, F., Guinand, B., 2012. Gene
674 flow at major transitional areas in sea bass (*Dicentrarchus labrax*) and the possible emergence of a hybrid
675 swarm. Ecol. Evol. 2(12), 3061-3078.
676 Sangiao-Alvarellos, S., Arjona, F.J., Martín del Río, M.P., Míguez, J.M., Mancera, J.M., Soengas, J.L.,
677 2005. Time course of osmoregulatory and metabolic changes during osmotic acclimation in *Sparus*
678 *auratus*. J. Exp. Biol. 208(22), 4291-4304.
679 Sardella, B.A., Matey, V., Cooper, J., Gonzalez, R.J., Brauner, C.J., 2004. Physiological, biochemical and
680 morphological indicators of osmoregulatory stress in `California' Mozambique tilapia (*Oreochromis*
681 *mossambicus*× *O. urolepis hornorum*) exposed to hypersaline water. J. Exp. Biol. 207(8), 1399-1413.
682 Schmidt-Nielsen, B., Renfro, J., 1975. Kidney function of the American eel *Anguilla rostrata.* Am. J.
683 Physiol. 228(2), 420-431.
684 Scott, G.R., Rogers, J.T., Richards, J.G., Wood, C.M., Schulte, P.M., 2004. Intraspecific divergence of
685 ionoregulatory physiology in the euryhaline teleost *Fundulus heteroclitus*: possible mechanisms of
686 freshwater adaptation. J. Exp. Biol. 207(19), 3399-3410.
687 Sunde, J., Tamario, C., Tibblin, P., Larsson, P., Forsman, A., 2018. Variation in salinity tolerance
688 between and within anadromous subpopulations of pike (*Esox lucius*). Sci. Rep. 8(1), 22.
689 Tang, C.H., Wu, W.Y., Tsai, S.C., Yoshinaga, T., Lee, T.H., 2010. Elevated Na^+/K^+-ATPase responses
690 and its potential role in triggering ion reabsorption in kidneys for homeostasis of marine euryhaline
691 milkfish (*Chanos chanos*) when acclimated to hypotonic fresh water. J. Comp. Physiol. B 180(6), 813-
692 824.
693 Tingaud-Sequeira, A., Calusinska, M., Finn, R.N., Chauvigné, F., Lozano, J., Cerdà, J., 2010. The
694 zebrafish genome encodes the largest vertebrate repertoire of functional aquaporins with dual paralogy
695 and substrate specificities similar to mammals. BMC Evol. Biol. 10(1), 38.
696 Tipsmark, C.K., Mahmmoud, Y.A., Borski, R.J., Madsen, S.S., 2010a. FXYD-11 associates with Na^+-K^+-
697 ATPase in the gill of Atlantic salmon: regulation and localization in relation to changed ion-regulatory
698 status. Am. J. Physiol. 299(5), R1212-1223.
699 Tipsmark, C.K., Sørensen, K.J., Madsen, S.S., 2010b. Aquaporin expression dynamics in osmoregulatory
700 tissues of Atlantic salmon during smoltification and seawater acclimation. J. Exp. Biol. 213(3), 368-379.
701 Tomy, S., Chang, Y.M., Chen, Y.H., Cao, J.C., Wang, T.P., Chang, C.F., 2009. Salinity effects on the
702 expression of osmoregulatory genes in the euryhaline black porgy *Acanthopagrus schlegeli*. Gen. Comp.
703 Endocrinol. 161(1), 123-132.
704 Vandeputte, M., Gagnaire, P.A., Allal, F., 2019. The European sea bass: a key marine fish model in the
705 wild and in aquaculture. Anim. Genet. 50(3), 195-206.
706 Vandesompele, J., De Preter, K., Pattyn, F., Poppe, B., Van Roy, N., De Paepe, A., Speleman, F., 2002.
707 Accurate normalization of real-time quantitative RT-PCR data by geometric averaging of multiple
708 internal control genes. Genome Biol. 3(7), Research0034.
709 Varsamos, S., Wendelaar Bonga, S.E., Charmantier, G., Flik, G., 2004. Drinking and Na^+/K^+ ATPase
710 activity during early development of European sea bass, *Dicentrarchus labrax*: Ontogeny and short-term
711 regulation following acute salinity changes. J. Exp. Mar. Biol. Ecol. 311(2), 189-200.
712 Yang, W.K., Kang, C.K., Hsu, A.D., Lin, C.H., Lee, T.H., 2016. Different modulatory mechanisms of
713 renal FXYD12 for Na^+-K^+-ATPase between two closely related medakas upon salinity challenge. Int. J.
714 Biol. Sci. 12(6), 730-745.
715 Yilmaz, H.A., Turkmen, S., Kumlu, M., Eroldogan, O.T., Perker, N., 2020. Alteration of growth and
716 temperature tolerance of European sea bass (*Dicentrarchus labrax*) in different temperature and salinity
717 combinations. Turk. J. Fish. Aquat. Sc. 20(5), 331-340.

718

719

720 Table 1. Morphometric parameters, muscle water content and plasma ion parameters in Mediterranean (M) and
721 Atlantic (A) European sea bass maintained in seawater (SW) and hypersaline water (HW). FL, mean fork length; W,
722 mean body wet weight; CF, condition factor; MWC, muscle water content. Different letters denote significant
723 differences between groups (two-way Anova followed by Tukey's test, $P < 0.05$, means ± SD, N = 12).

724

Conditions	FL (cm)	W(g)	CF (g/cm3)	MWC
MSW	11.64±1.38^{a}	18.30±6.49^{b}	0.98±0.08^{a}	73.37±1.68^{a}
MHW	13.34±0.93^{a}	24.69±4.37^{ab}	1.04±0.16^{a}	71.80±1.74^{a}
ASW	12.40±2.36^{a}	21.89±10.4^{ab}	0.99±0.16^{a}	72.18±1.70^{a}
AHW	12.76±1.99^{a}	27.65±13.51^{a}	1.09±0.09^{a}	71.89±1.24^{a}

725

726

727 Table 2. Primer sequences used for qPCR in this study. F: forward primer; R: reverse primer. Sequences ID
728 indicates gene sequences from the sea bass genome or Genbank identification numbers when available.

Sequences ID	Target gene	Primer name	Sequence (from 5′ to 3′)	Amplicon Size	Efficiency
KP400258	*nka α1a*	*nka α1a*-F	CCTCAGATGGCAAGGAGAAG	146	2.003
		nka α1a-R	CCCTGCTGAGATCGGTTCC		
KP400259	*nka α1b*	*nka α1b*-F	AGCAGGGCATGAAGAACAAG	204	2.048
		nka α1b-R	CCTGGGCTGCGTCTGAGG		
DLAgn_00006940	*aqp 1a*	*aqp 1a*-F	CTGCCTGGGACACTTGGCAGC	194	1.99
		aqp 1a-R	TCTCAGGGAAGTCATCAAA		
DLAgn_00006960	*aqp 1b*	*aqp 1b*-F	CGGACCAGCCGTGATACAGG	147	1.92
		aqp 1b-R	AGCAGGACGTTCCAGCCCG		
DLAgn_00099310	*aqp 8aa*	*aqp 8aa*-F	TGCTTCCTTTGGCGGTGCC	199	2.110
		aqp 8aa-R	CAACATCCCTCCAGCAAGT		
DLAgn_00099320	*aqp 8ab*	*aqp 8ab*-F	AGCCGCCTGTGTCCAAACCTCC	198	1.951
		aqp 8ab-R	CATAACCGCCACCATCACTG		
DLAgn_00189570	*aqp 8b*	*aqp 8b*-F	TGTCAGTTGGTCGGAGGAGTGC	282	1.809
		aqp 8b-R	CAGACAAGTGCCAGATACATCT		
DLAgn_00202560	*aqp 10b*	*aqp 10b*-F	AGCGGCTACGCACTTAAC	150	1.911
		aqp 10b-R	CAGTGTTCCCAACAGCGCC		
FM004681	*fau*	*fau*-F	GACACCCAAGGTTGACAAGCAG	150	1.979
		fau-R	GGCATTGAAGCACTTAGGAGTTG		
AJ866727	*ef1α*	*ef1α*-F	GGCTGGTATCTCTAAGAACG	239	1.982
		ef1α-R	CCTCCAGCATGTTGTCTCC		
DLAgn_00023060	*l13*	*l13*-F	TCTGGAGGACTGTCAGGGGCATGC	148	2.012
		l13-R	AGACGCACAATCTTGAGAGCAG		

729

730

731 Table 3: Two-way Anova results of data with salinity and genetic lineage as the main factors. ns: not
732 significant, *P<0.05, ** P <0.01, *** P <0.001, **** P <0.0001. N=10-12 per condition. ns: not
733 significant.

	Interaction	Salinity	Lineage
Blood osmolality	**	****	***
Muscle water content	ns	ns	ns
Plasma sodium	ns	****	****
Plasma chloride	ns	****	ns
Glomerulus area	ns	****	**
Glomerulus perimeter	ns	****	***
nka α1a mRNA	ns	**	**
nka α1b mRNA	ns	*	ns
aqp 1a mRNA	ns	***	**
aqp1b mRNA	ns	ns	ns
aqp8b mRNA	ns	ns	*
NKA activity	ns	****	**
NKA abundance	****	****	****

734

735

736

737 Figure legends

738 Fig. 1. Blood osmolality (A), plasma sodium (B) and chloride (C) levels in Mediterranean (M) and
739 Atlantic (A) European sea bass maintained in seawater (SW) and hypersaline water (HW). Data are
740 represented as the median, first and third quartile (box), minimum and maximum values. Different letters
741 indicate significant differences between conditions (two-way ANOVA followed by Tukey's multiple
742 comparisons test, P <0.05, N=10–12).

743

744 Fig. 2. Kidney sections of Mediterranean (A, B) and Atlantic (C, D) European sea bass maintained in
745 seawater (SW) (A, C) and hypersaline water (HW) (B, D). Kidney glomerulus area (E) and perimeter (F)
746 are represented in three fish per condition. Measurements from a same animal are indicated by a same
747 color. Data are represented as the mean +/-SD. Different letters denote significant differences between
748 groups (two-way ANOVA followed by Tukey's multiple comparisons test, P < 0.05, N=11). CT,
749 collecting tubule; PT, proximal tubule; G, glomerulus. Scale bars: 50 µm.

750

751 Fig. 3. Relative *nka α1a* (A), *nka α1b* (B), *aqp 1a* (C), *aqp 1b* (D) and *aqp 8b* (E) mRNA expression in
752 the posterior kidney of Mediterranean (M) and Atlantic (A) European sea bass maintained in seawater
753 (SW) and hypersaline water (HW). The expression has been normalized according to the expression of
754 elongation factor 1α (*ef1α*), ribosomal protein (*l13*) and ribosomal protein S30 fusion gene (*fau*). Data are
755 represented as the median, first and third quartile (box), minimum and maximum values. Different letters
756 denote significant differences between groups (two-way ANOVA followed by Tukey's test, P < 0.05, N =
757 10–12).

758

Fig. 4. Immunoblots probed with a monoclonal antibody α5 to Na^+/K^+-ATPase (NKA) α subunit showed a single band in the posterior kidney at a molecular weight at around 105 kDa (A). The marker (Ma) is indicated on the left of the immunoblot. Relative NKA α-subunit abundance (B) and NKA activity (C) was measured in the posterior kidney of Mediterranean (M) and Atlantic (A) European sea bass maintained in seawater (SW) and hypersaline water (HW). Different letters denote significant differences between groups (two-way ANOVA followed by Tukey's test, $P < 0.05$, N = 10). Data are represented as the median, first and third quartile (box), minimum and maximum values.

Fig. 5. Double immunofluorescent staining of AQP1a (Aquaporin 1a; green) (A, C, E) and NKAα (Na^+/K^+-ATPase α; red) (B, C, D) in posterior kidneys of Mediterranean European sea bass maintained in seawater (MSW). Merged image of AQP1a and NKAα and DAPI-counterstained nuclei (C). The asterisks (*) indicate proximal tubules (II) with light AQP1a staining and basolateral NKAα as well as an apical brush border (arrowhead). The pluses (+) indicate another type of proximal tubules (I) with a light basolateral NKA staining and a strong basolateral AQP1a. Arrows show distal tubules that, as collecting tubules (CT) show strong NKAα staining in the whole cell and faint AQP1a. Glomeruli (G) are not immunolabeled. Scale bars: 50 μm (A-C), 20 μm (D, E).

Fig. 6. Double immunostaining of AQP1a (Aquaporin 1a, green) (A, B, D) and NKAα (Na^+/K^+-ATPase α, red) (C, D) of a collecting duct in Atlantic European sea bass maintained in seawater (ASW). The dashed box shown in (A) represents the enlarged portion shown in (B). A nearly not detectable staining of AQP1a is observed in the subapical part of the cells lining the collecting duct (B: arrow). NKAα shows a strong staining in the whole cells. Nuclei are counterstained with DAPI (A, B, D). Scale bars: 20 μm (A, C, D), 10 μm (B).

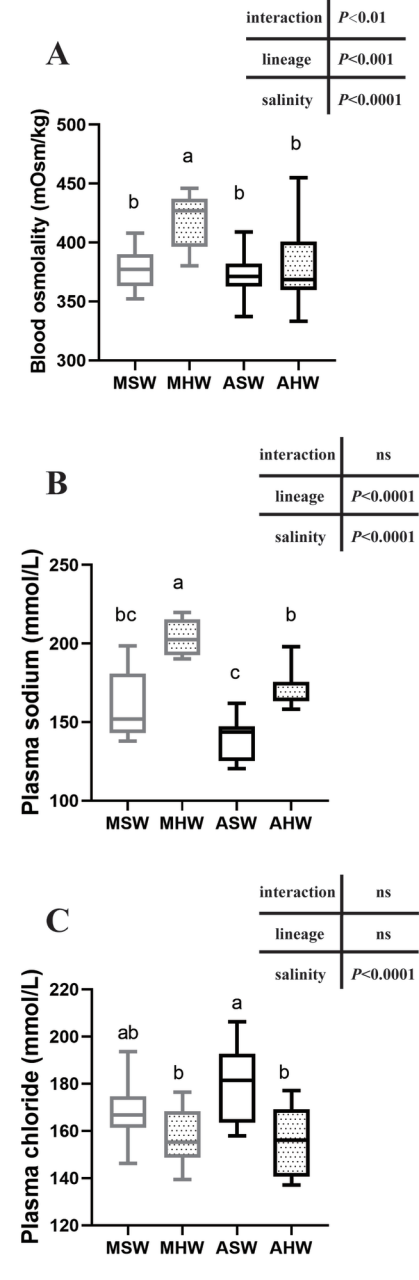
A
interaction
P<0.01
lineage
P<0.001
salinity
P<0.0001
Blood osmolality (mOsm/kg)
500
450
400
350
300
a
b
b
b
MSW MHW ASW AHW
B
interaction
ns
lineage
P<0.0001
salinity
P<0.0001
Plasma sodium (mmol/L)
250
200
150
100
bc
a
c
b
MSW MHW ASW AHW
C
interaction
ns
lineage
ns
salinity
P<0.0001
Plasma chloride (mmol/L)
220
200
180
160
140
120
ab
b
a
b
MSW MHW ASW AHW

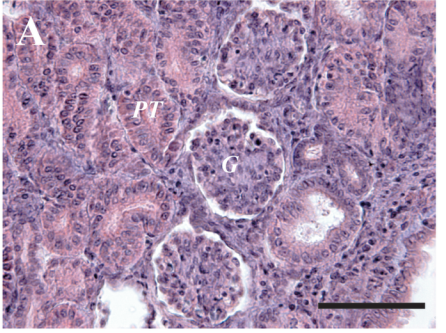

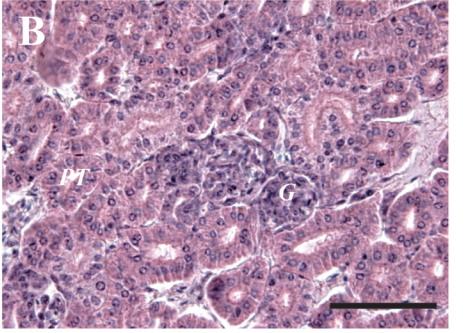

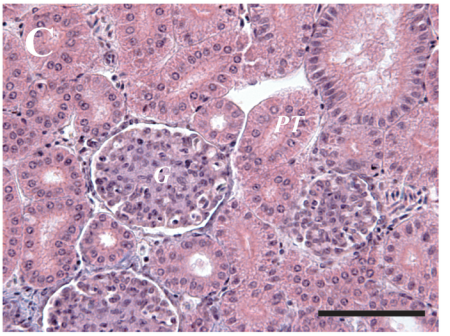

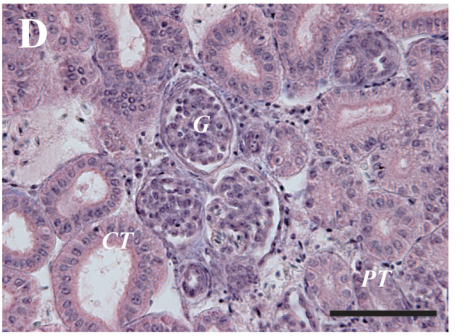

E

interaction	ns
lineage	*P*<0.01
salinity	*P*<0.0001

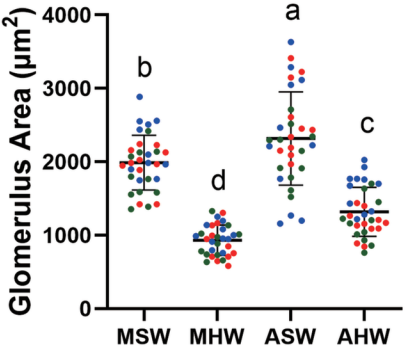

F

interaction	ns
lineage	*P*<0.001
salinity	*P*<0.0001

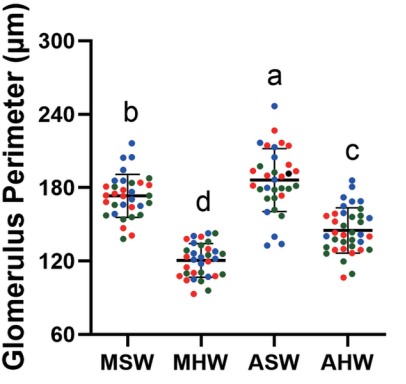

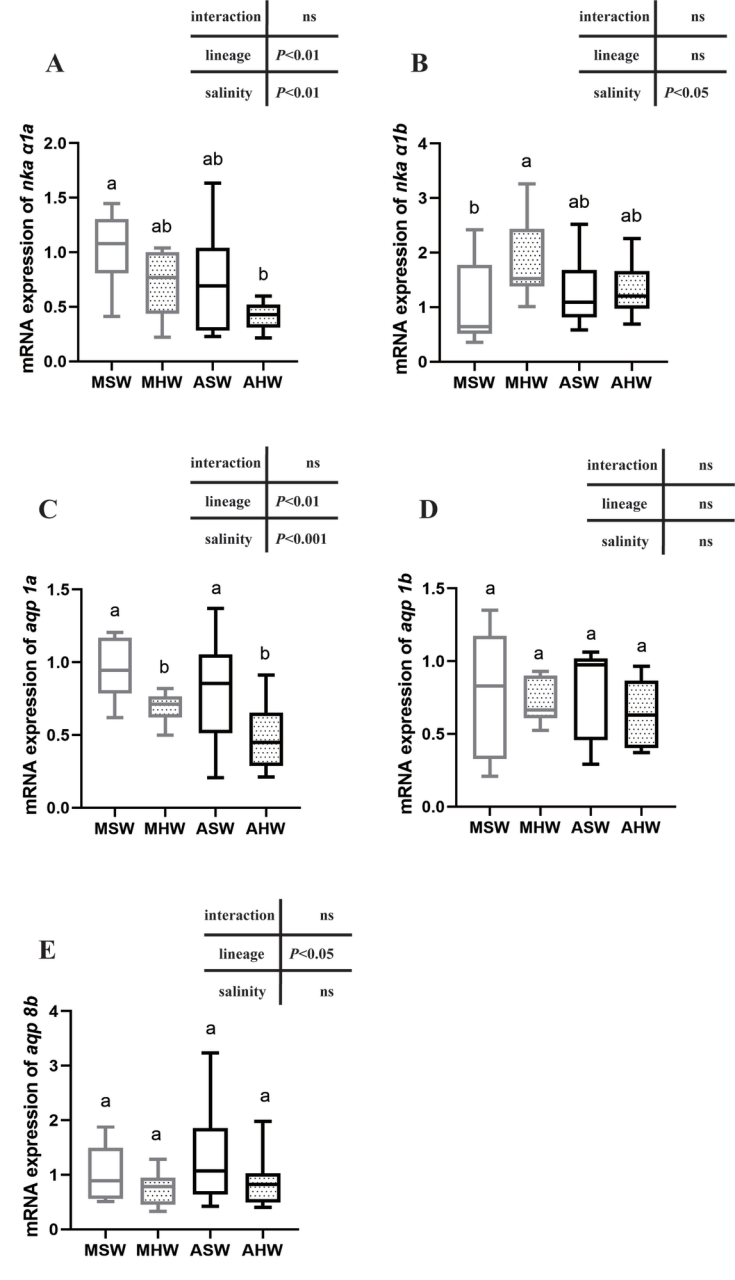
A
interaction ns
lineage P<0.01
salinity P<0.01
mRNA expression of nka α1a
2.0
1.5
1.0
0.5
0.0
a
ab
ab
b
MSW MHW ASW AHW
B
interaction ns
lineage ns
salinity P<0.05
mRNA expression of nka α1b
4
3
2
1
0
b
a
ab
ab
MSW MHW ASW AHW
C
interaction ns
lineage P<0.01
salinity P<0.001
mRNA expression of aqp 1a
1.5
1.0
0.5
0.0
a
b
a
b
MSW MHW ASW AHW
D
interaction ns
lineage ns
salinity ns
mRNA expression of aqp 1b
1.5
1.0
0.5
0.0
a
a
a
a
MSW MHW ASW AHW
E
interaction ns
lineage P<0.05
salinity ns
mRNA expression of aqp 8b
4
3
2
1
0
a
a
a
a
MSW MHW ASW AHW

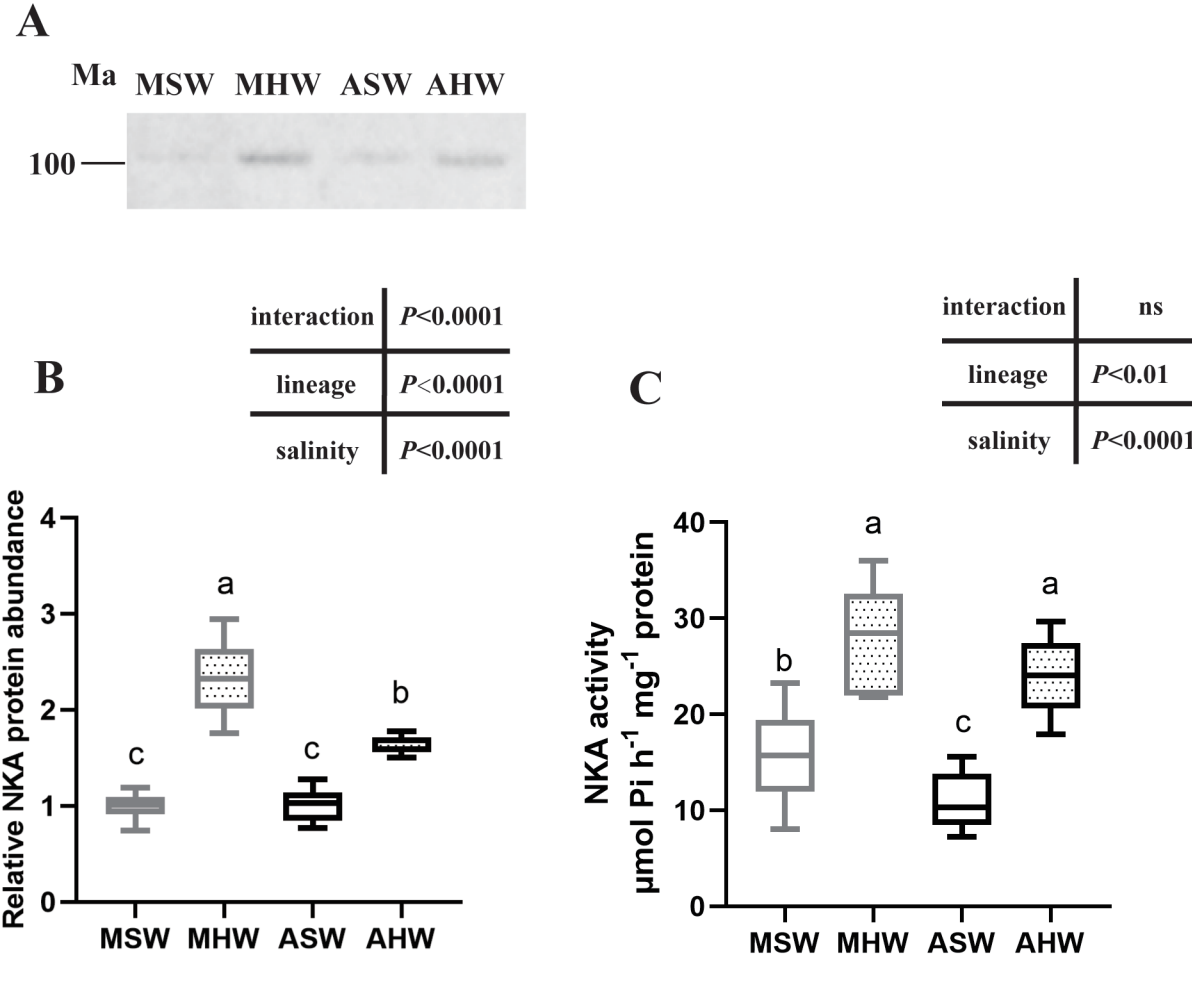
A
Ma
MSW
MHW
ASW
AHW
100
B
interaction
P<0.0001
lineage
P<0.0001
salinity
P<0.0001
Relative NKA protein abundance
0
1
2
3
4
c
a
c
b
MSW
MHW
ASW
AHW
C
interaction
ns
lineage
P<0.01
salinity
P<0.0001
NKA activity
μmol Pi h-1 mg-1 protein
0
10
20
30
40
b
a
c
a
MSW
MHW
ASW
AHW

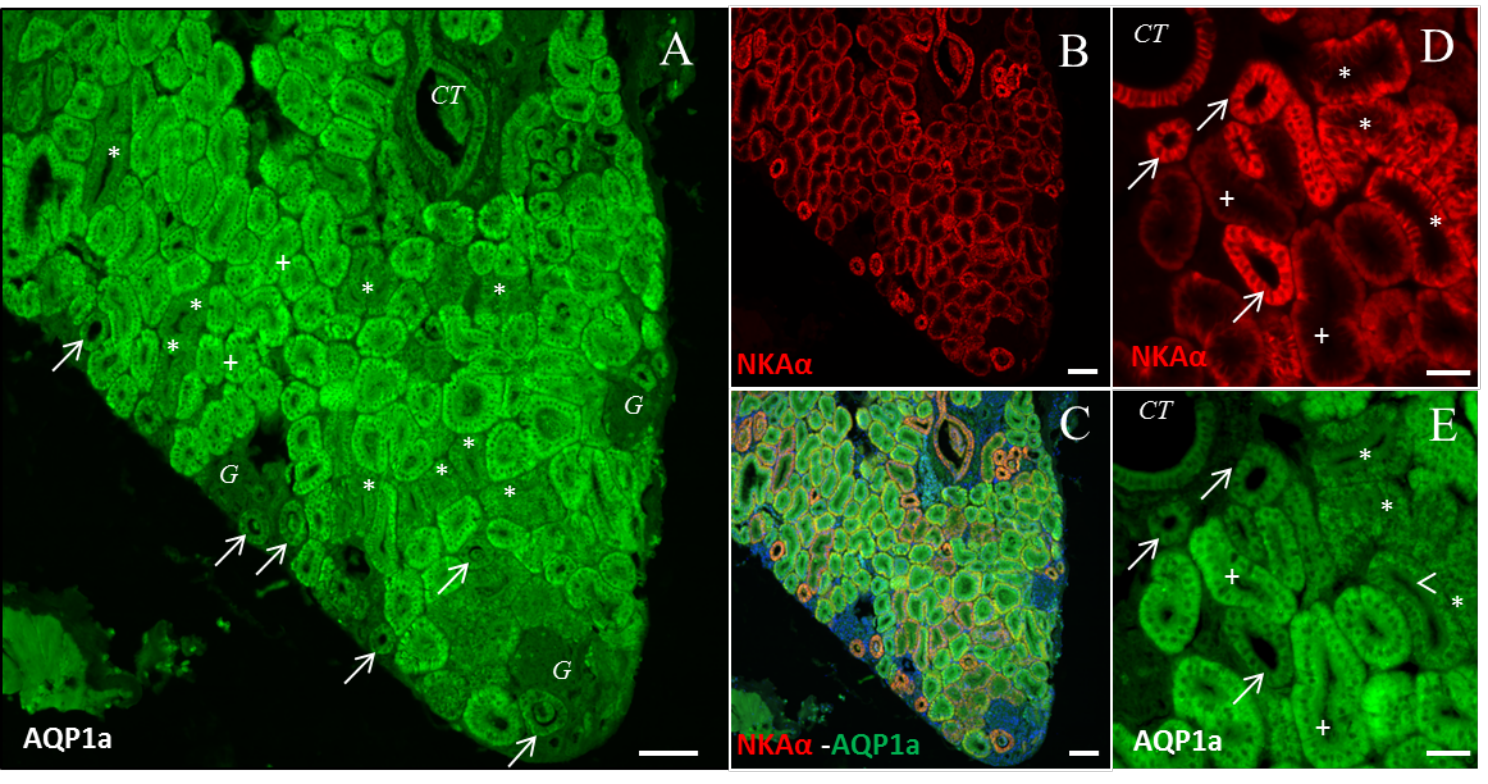
A
CT
G
G
G
AQP1a
B
NKAα
C
NKAα -AQP1a
D
CT
NKAα
E
CT
AQP1a

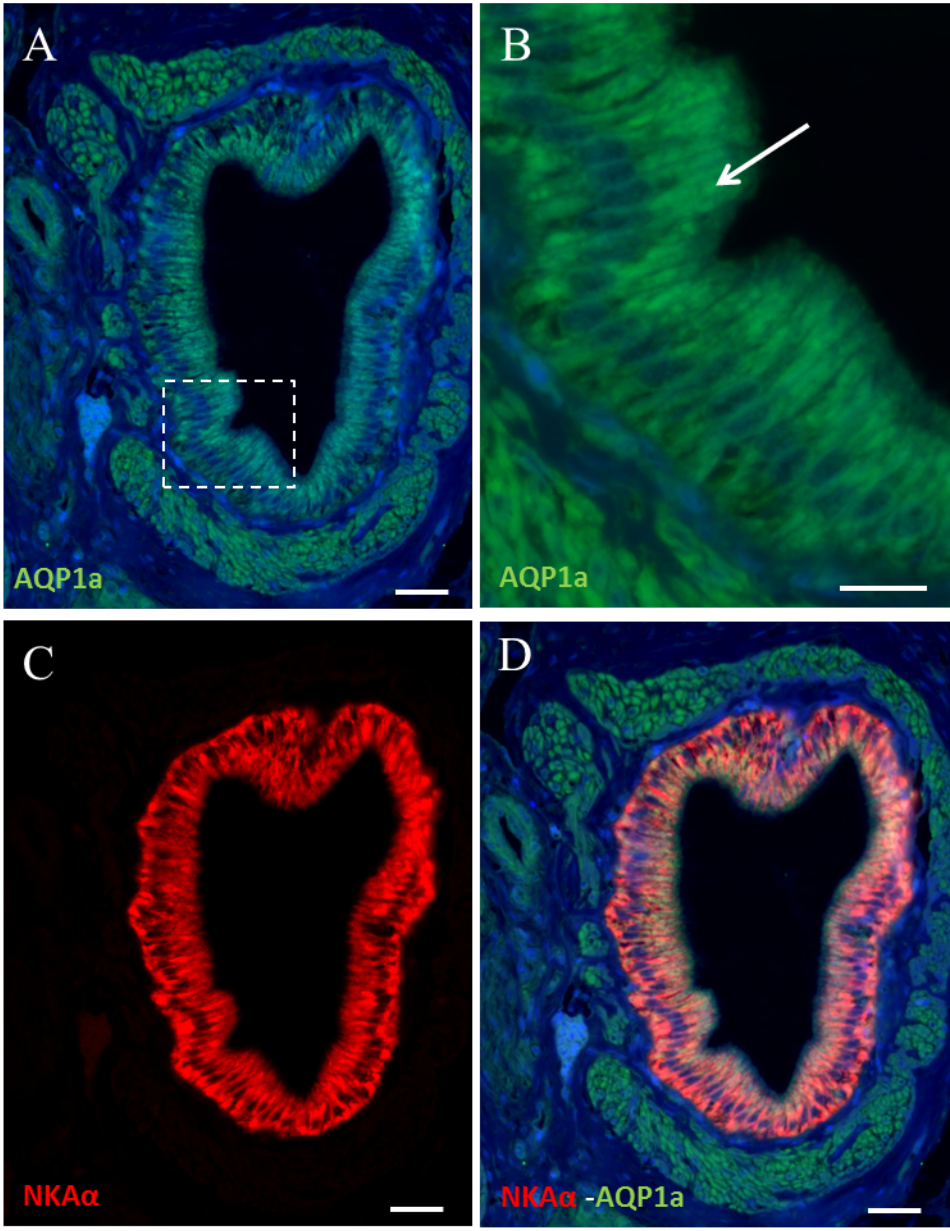
A
AQP1a
B
AQP1a
C
NKAα
D
NKAα -AQP1a